JVI Accepted Manuscript Posted Online 10 January 2018
J. Virol. doi:10.1128/JVI.01766-17

1 **REVISED**

2

3 **Dengue virus selectively annexes endoplasmic reticulum-associated translation**

4 **machinery as a strategy for co-opting host cell protein synthesis**

5

6 David W. Reid,[a] Rafael K. Campos,[b,c] Jessica R. Child,[a] Tianli Zheng,[a] Kitti Wing Ki
7 Chan[d,e], Shelton S. Bradrick,[b], Subhash G. Vasudevan[d,e], Mariano A. Garcia-Blanco,[b,d]
8 and Christopher V. Nicchitta[a]#

9

10 Department of Cell Biology, Duke University Medical Center, Durham, NC, USA[a];
11 Department of Biochemistry and Molecular Biology, University of Texas Medical Branch,
12 Galveston, TX, USA[b]; Department of Molecular Genetics and Microbiology, Duke
13 University Medical Center, Durham, NC, USA[c]; Programme in Emerging Infectious
14 Diseases, Duke-NUS Medical School, Singapore[d,] Department of Microbiology, Yong
15 Loo Lin School of Medicine, Singapore[e]

16

17 **Running title:** Dengue co-opts ER-associated translation

18

19 **#Address correspondence to:**

20 Christopher V. Nicchitta, PhD:

21 christopher.nicchitta@duke.edu

22

23 **Abstract:** 250 words

24 **Text:** 7,364 words

Abstract

A primary question in Dengue virus (DENV) biology is the molecular strategy for recruitment of host cell protein synthesis machinery. Here we combined cell fractionation, ribosome profiling, and RNA-seq to investigate the subcellular organization of viral genome translation and replication as well as host cell translation and its response to DENV infection. We report that throughout the viral life cycle, DENV (+) and (-) strand RNAs were highly partitioned to the endoplasmic reticulum (ER), identifying the ER as the primary site of DENV translation. DENV infection was accompanied by an ER compartment-specific remodeling of translation, where ER translational capacity was subverted from host transcripts to DENV (+) strand RNA, particularly at late stages of infection. Remarkably, translation levels and patterns in the cytosol compartment were only modestly affected throughout the experimental time course of infection. Comparisons of ribosome footprinting densities of the DENV (+) strand RNA and host mRNAs indicated that DENV (+) strand RNA was only sparsely loaded with ribosomes. Combined, these observations suggest a mechanism where ER-localized translation and translational control mechanisms, likely *cis*-encoded, are used to repurpose the ER for DENV virion production. Consistent with this view, we found ER-linked cellular stress response pathways commonly associated with viral infection, namely the interferon response and unfolded protein response, to be only modestly activated during DENV infection. These data support a model where DENV reprograms the ER protein synthesis and processing environment to promote viral survival and replication, while minimizing the activation of anti-viral and proteostatic stress response pathways.

Importance

DENV, a prominent human health threat with no broadly effective or specific treatment, depends on host cell translation machinery for viral replication, immune evasion, and virion biogenesis. The molecular mechanism by which DENV commandeers the host cell protein synthesis machinery and the subcellular organization of DENV replication and viral protein synthesis is poorly understood. Here we report that DENV has an almost exclusively ER-localized life cycle, with viral replication and translation largely restricted to the ER. Surprisingly, DENV infection largely affects only ER-associated translation, with relatively modest effects on host cell translation in the cytosol. DENV RNA translation is very inefficient, likely representing a strategy to minimize disruption of ER proteostasis. Overall these findings demonstrate that DENV has evolved an ER-compartmentalized life cycle and thus targeting the molecular signatures and regulation of the DENV-ER interaction landscape may reveal strategies for therapeutic intervention.

Introduction

The synthesis of viral proteins, which function in viral replication, evasion of immune defenses, and virion biogenesis, is wholly dependent on host cell translation machinery. Reflecting this need, viruses have evolved diverse strategies to out-compete cellular mRNAs and co-opt host translation capacity. Some viruses have evolved mRNAs that are translated by alternative mechanisms (e.g., IRES mediated, cap-independent translation initiation) and genes that modify or inactivate host cell factors required for cap-dependent host translation, thus providing mechanisms for viral RNAs to efficiently recruit ribosomes (1-6). Other viruses encode nucleases that specifically degrade host mRNAs, thereby significantly decreasing the competition of cellular translation activity (7). Yet others produce mRNAs that can, by nature of their extraordinary translation efficiency and/or high levels, outcompete most cellular mRNAs (8-10). As viral replication and viral protein synthesis is strictly dependent on the host cell translation machinery, understanding the mechanisms by which viruses promote translation of their RNAs within cells provides not only understanding of viral pathogenic mechanisms but also insights into host cell regulation of protein synthesis (11).

The mechanism by which Dengue virus (DENV), a member of the Flavivirus genus of RNA viruses and a prominent human pathogen, usurps host cell protein synthesis is largely unknown. Like all members of the genus *Flavivirus*, DENV contains an enveloped 5' m^7GpppA-capped (+)-sense RNA genome with a nonpolyadenylated 3' untranslated region (UTR). The DENV 10.7 kb genome encodes a single polyprotein which is post-translationally cleaved into three structural (capsid [C], pre-membrane/membrane [prM/M], and envelope [E]) and seven nonstructural (NS1, NS2A,

NS2B, NS3, NS4A, NS4B, and NS5) proteins required for viral replication and inactivation of antiviral cellular pathways (12-14). Neither the structural nor nonstructural proteins are known to modify or compete with the cellular translation machinery. Indeed, earlier studies report little to no effect of DENV infection on total host cell protein synthesis (15, 16). Translation initiation of the DENV (+) strand RNA is thought to occur primarily through a canonical cap-dependent mechanism (17), although alternative strategies have been described when cap-dependent translation is inhibited (15).

DENV enters cells through receptor-mediated endocytosis (18) and gains access to the cytosol compartment following fusion of the viral envelope with the endosomal membrane. Having gained access to the cytosol, the viral genome then undergoes cycles of translation and replication that can produce upwards of 10,000 infectious particles per cell within 48 hours (19). Prior to the onset of viral replication, synthesis of the RNA-dependent RNA polymerase NS5, the RNA helicase NS3, and other NS proteins must occur, as these are required for assembly of the viral replication complex (20). Because (-) strand RNA synthesis and (+) strand translation compete for the same (+) strand template (21), the interplay between these two processes and their associated RNA structures is critical for optimal viral replication. Different long range RNA-RNA interactions appear to partition the genome between a linear form devoted to protein synthesis and a circular form focused on RNA transcription (22, 23), allowing for separation of these two processes in space and time.

DENV polyprotein and genome replication occurs in association with the endoplasmic reticulum (ER) (24). This intracellular membrane affiliation reflects both the nature of the polyprotein, which contains ca. twenty transmembrane domains and is dependent on

the ER protein translocation machinery for its biogenesis, and that many of the non-structural proteins, e.g. NS4A, behave as ER-resident membrane proteins and are principal components of ER-associated replication factories (24, 25). Correspondingly, DENV replication is highly sensitive to silencing or knock-out of host factors functioning in protein translocation and/or processing in the ER (26-28). Once the components of a viral particle have been synthesized, virions assemble and bud into the ER lumen, utilizing the secretory pathway to exit the cell (12).

Understanding how an ER-localized DENV (+) strand RNA serves as a template for temporally coordinated synthesis of both DENV (-) strand RNA and DENV proteins is important for understanding the DENV life cycle, yet our knowledge of these processes is limited. We considered this incomplete understanding in the context of our recent studies that point to distinct regulatory control of mRNA translation in the cytosol and ER (29-32) as well as transcriptome-wide functions for the ER-associated translation machinery in gene expression (30, 33). We thus paired ribosome profiling (34, 35) and RNA-Seq with biochemical cell fractionation (31, 36), to examine the subcellular organization of DENV translation through the viral life cycle. The overarching theme in the data is a DENV dependence on and selective modification of the ER-associated protein synthesis machinery. Three primary findings were revealed in this study. One, viral RNA, including the (-) strand replication template, and viral protein synthesis are wholly ER-compartmentalized. Second, DENV (+) strand RNA translation is highly inefficient relative to host cell mRNAs, suggesting a competition/selective capture mechanism for annexing host cell ER-associated ribosomes. Third, the host translational response to DENV infection is highly compartmentalized to the ER, as

most host ER-associated mRNAs are translationally suppressed, yet cytosolic host protein synthesis is relatively unchanged. Comparisons of transcriptome-wide changes in translation of host genes during DENV infection to the translational response evoked by the unfolded protein response (UPR) or treatment with interferon-β (IFN) demonstrated that the host translation response to DENV included both UPR and IFN response pathways, and revealed a subset of genes whose translation is up-regulated during DENV infection. Interesting, we report that previously identified essential host factors for DENV infection are not translationally up-regulated during infection, but are rather generally repressed. These findings demonstrate that DENV specifically annexes ER-associated ribosomes, sacrificing synthesis of specific host proteins to maximize viral replication.

Results

Tracking the subcellular compartmentalization of DENV genome replication and translation.

The DENV 10.7 Kb (+) strand RNA, which encodes both cytosolic and integral membrane proteins, accesses the cytosol early in infection and is subsequently localized to the endoplasmic reticulum (ER), where it's translation products assemble replication and virion biogenesis centers (37, 38). As a first step towards understanding the molecular strategies used by DENV to commandeer host cell translation, we examined subcellular RNA distributions and the translational status of both host cell mRNAs and DENV (-) and (+) strand RNAs through the viral life cycle (36, 39). In combining the cell fractionation protocol illustrated in **Fig.1A**, which efficiently separates the two primary protein synthesis compartments of the cell, with RNA-seq and ribosome profiling, we sought to determine how DENV infection impacts the subcellular distribution and translation of host cell mRNAs, as it captures mRNA translation capacity and secretory pathway function, the latter for the production and secretion of new virions. In these experiments, Huh-7 hepatocarcinoma cells were infected with DENV (serotype 2; strain New Guinea-C) at a multiplicity of infection (MOI) of 10. After one hour, the viral inoculum was removed and the cells cultured for 6, 12, 24, or 40 hours post infection (pi). At each time point, cells were fractionated using a sequential detergent-based fractionation method (**Fig. 1A**) (32, 36, 40). As illustrated, cells are first treated with a digitonin-supplemented physiological salts buffer, which selectively permeabilizes the plasma membrane and releases the cytosolic contents. The digitonin-extracted cells are then treated with n-dodecyl-β-D-maltoside (DDM)-supplemented

buffers to release ER-associated cellular components. Similar to data reported in prior studies (39, 41-46), the immunoblot data in **Fig. 1B** demonstrate that the fractionation protocol yields the efficient separation and recovery of cytosolic (e.g., GAPDH, tubulin) and ER-resident (e.g., ribophorin I, TRAPα) proteins, in both mock and DENV-infected cells. Note that DENV NS4B, an integral membrane protein, was wholly ER-associated in DENV-infected cells and absent from mock-infected cells (**Fig. 1B**). As expected, rRNAs (ribosomes) were recovered in both fractions, showing a modest ER-enrichment in mock-infected cells and an approximately equal subcellular distribution at 40 h post-infection (**Fig. 1C**). tRNAs, in contrast, were largely recovered in the cytosol fraction (**Fig. 1C**). The RNA component of the two subcellular fractions was analyzed by ribosome profiling (35), to assess mRNA translation status, and RNA-seq, to profile mRNA transcriptome composition (**Table S1**).

As depicted in **Fig. 2A**, the 40 hour time course captured the major phases of the DENV life cycle. DENV (+) strand RNA levels mirrored a logistic growth curve, with an apparent lag phase extending to approximately 12 hours followed by a replication phase. DENV (-) strand RNA levels, by contrast, steady increased until 24 hours post infection, followed by a decline. The relative levels of the DENV (+) strand, determined from the deep sequencing datasets, were approximately an order of magnitude higher than the DENV (-) strand throughout infection. We calculated the relative rates of (-) and (+) strand DENV RNA synthesis from the changes in RNA levels (**Fig. 2B).** Under the indicated experimental conditions, the peak rate of increase for the (+) strand RNA occurred between 12 and 24 h post-infection, with a doubling time of 20 min (±3.8 min). It should be noted that at an MOI of 10, each cell was likely exposed to ≥ 1,000 DENV

genomes, many of which could be defective in typical infections (47), thus likely lowering the calculated initial (+) strand synthesis rate. The pattern of change in (-) strand RNA levels differed markedly from (+) strand RNA, peaking early in infection and dropping throughout the remainder of the time course. The (-) strand RNA produced early in infected presumably serves as a subsequent template for robust (+) strand synthesis. These data identify an important temporal transition in the viral life cycle, where early periods of infection are weighted to (-) strand synthesis and later time periods to (+) strand synthesis and virion production.

We next investigated the subcellular localization of (-) and (+) strand RNA, as well as (+) strand translation, over the time course of infection (**Fig. 2C**). Both (-) and (+) strand RNAs were highly partitioned to the ER, where the (-) strand RNA remained almost entirely ER-bound throughout the time course despite not being translated. This finding may reflect localization of the (-) strand to ER-associated replication center and association with ER-associated template (+) strand. While the (+) strand is mostly ER-bound early in the infection, at late time points a discernible increase of (+) strand RNA in the cytosol was observed. The precise subcellular disposition of this fraction of (+) RNA is, however, not known, as at these late time points (+) strand RNA that scored as cytosolic includes maturing viral particles packaged within secretory pathway transport vesicles. In support of this interpretation, the translation of viral proteins remained highly ER-enriched at all time points, which is consistent with non-virion complexed (+) strand RNA being largely ER-associated throughout the experimental time course (**Fig. 2C**).

In addition to defining the subcellular locale of DENV translation, the ribosome profiling data allowed assessment of the translation status of the (+) RNA. Because DENV first

accesses the cytosol compartment in early infection, and subsequently uses the endoplasmic reticulum (ER) as a platform for virion production, we calculated the translation efficiency of the DENV (+) strand RNA in both the cytosolic and ER compartments, where translation efficiency is defined as the ribosome density within the coding sequence normalized to the level of the corresponding mRNA and is a proxy for mRNA translational status. The translation efficiency of cytosolic (+) strand RNA was low throughout the experimental time course. Intriguingly, for ER-bound DENV (+) strand RNA, translation efficiency is relatively low at the 6 h time point, but increases by 12h post infection where it is sustained (data not shown). This period of relatively low translation efficiency on the ER overlaps with the period of high minus-strand synthesis rates, suggesting that at early infection, (+) strand translation is suppressed in favor of RNA replication. This transition may reflect a regulated transition from a primarily circularized, replication-dedicated (+) strand structure to a linearized, translationally-competent structure, as suggested previously (23, 48). Notably, even at the time points where DENV (+) strand RNA translation efficiency was highest, the relative translation efficiency was quite low relative to the host mRNA transcriptome, scoring in the bottom 5th percentile (**Fig. 2D**). As we do not know the relative fraction of DENV (+) strand RNA engaged in transcription vs. translation, and whether the two processes are biochemically exclusive, the precise translation efficiency score cannot be stated with certainty. Nonetheless, these data suggest that the DENV (+) strand RNA is an intrinsically weak substrate for translation. The inefficiency of DENV translation may reflect, at least in part, its highly structured 5' UTR (49-51). There was essentially no detectable translation of the (-) strand RNA (**Fig. 2D**).

Ribosome footprinting analysis of DENV (+) strand RNA translation reveals intragenic variations in ribosome loading.

To gain insight into the translational dynamics of the DENV (+) strand RNA, we examined the positional arrangement of the ribosome profiling reads over the ~ 10.3 Kb CDS at each time point in the experimental time course of infection (**Fig. 3A,C**). As depicted in **Fig. 3A**, ribosomes were broadly distributed along the CDS, with the prominent peaks and valleys that are typical of ribosome profiling data (35). The ribosome distribution pattern was largely unchanged over the experimental time course, suggesting that synthesis of a composite balance of structural and non-structural proteins is sustained throughout the infection cycle, which would be expected given the single ORF (**Fig. 3A-C**). In support of this conclusion, Pearson's correlation coefficients for ribosome densities between biological replicates were indistinguishable from comparisons between time points (r=0.85 for replicates vs. 0.87 for comparisons; *p*-value=0.35 by two-tailed Student's t-test).

We next examined ribosome densities relative to the established N- and C-termini boundaries of the encoded proteins of the polyprotein, as a measure of intragenic translational variation (**Fig. 3C).** Such analyses are useful for defining alternative open reading frames, multiple ORFs, and ribosomal frame-shifting, as recently reported for the coronavirus, MHV, a (+) strand RNA virus (52). Programmed ribosomal frame shifting and/or multiple ORFs are not known to be strategies utilized by DENV (53, 54). Evident, however, are intragenic variations in ribosome density, where ribosome densities are lowest in the intragenic region encoding capsid and highest for the regions encoding NS2B, NS4B and NS5. Though relatively modest (net change < 1.5 fold) the

intragenic variations in ribosome densities could arise through *cis*-encoded translational regulation, perhaps coupled to the ordered co-translational proteolytic processing of the DENV polyprotein into individual proteins (55, 56). The variations in ribosome density might also reflect a molecular strategy to compensate for differential stabilities of the processed proteins and so will require a detailed understanding of both intragenic ribosomal processivity and the stability/turnover rates of the individual processing-derived proteins to determine biological relevance.

A high number of RNA-seq reads mapped to the 3' UTR. These reads increased with time of infection and thus likely reflect production of the subgenomic flaviviral RNA (sfRNA) (57) (**Fig. 4**). This interpretation is supported by the lack of similar changes in 5' UTR RNA-seq map read densities as a function of time of infection. The sfRNA is a product of degradation of the viral genome by 5` to 3` exonucleases. The functions of the sfRNA in viral infection remain to be fully elucidated, but it is known to play a role in suppressing interferon stimulated genes expression, thus helping the virus evade the immune system. In contrast to the full DENV (+) strand RNA, the sfRNA was not highly enriched on the ER, consistent with previous work demonstrating functions for the sfRNA in the regulation of cytosolic anti-viral immunity factors (**Fig. 4B**) (58). Ribosome profiling reads mapping to the untranslated regions (UTR), particularly the 3' UTR were also obtained (**Fig. 3A**), but they were at a much lower density and their size distribution was discernibly different from other genes, suggesting that they likely represent nuclease protection by means other than ribosomes (e.g., RNA binding proteins, highly structured/nuclease resistant RNA domains), rather than translation (**Fig. 4C**).

DENV infection predominantly remodels translation on the ER compartment.

With the ribosome profiling data demonstrating that DENV (+) strand RNA translation was almost entirely localized to ER-bound ribosomes (**Fig. 2C**), we next examined the impact of viral RNA translation on global host cell protein synthesis, via the cell fractionation methodology introduced above. We first compared the relative abundance of ribosome footprint reads on ER-targeted mRNAs (mRNAs which encode an N-terminal hydrophobic signal sequence and/or transmembrane domains and are localized to the ER for translation and translocation) and cytosolic protein-encoding mRNAs (mRNAs which do not encode a signal sequence or transmembrane domain and are abundantly translated in the cytosol) (31, 33, 59, 60) (**Fig. 5A**). As illustrated in **Fig. 5A**, it was apparent that DENV infection resulted in time-dependent decrease in the translation of host ER-targeted mRNAs, beginning early in infection and progressing throughout the experimental infection period. In contrast, the translation of cytosol-encoding mRNAs was, on average, unchanged. As illustrated in **Fig. 5B**, analysis of the total RNA-seq datasets revealed that the levels of mRNAs encoding both ER-targeted and cytosolic proteins decreased somewhat over the course infection. The Ribo-Seq and RNA-seq analyses thus indicate that reductions in both ribosome loading and overall mRNA levels contribute to a reduction of total translation on the ER.

As previously reported, cytoplasmic protein-encoding mRNAs are broadly represented on the ER, though enriched in the cytosol compartment (31, 33, 59, 60). In the ER compartment specifically, the host ER-targeted mRNA cohort showed a 50% reduction in translation levels (**Fig. 5C**), whereas ER-associated cytosol-encoding mRNAs were only modestly altered (ca. 15% (**Fig. 5D**), indicating that the impact of DENV on ER-

associated translation was largely restricted to ER-associated secretory/membrane protein-encoding mRNAs. Because the DENV (+) strand RNA encodes ca. twenty transmembrane domains, its polyprotein translation product would be expected to compete with the translation products of host ER-targeted mRNAs for access to the protein translocation machinery. We thus further examined the impact of DENV infection on the translation of ER-targeted host mRNAs. To obtain a quantitative estimate of the impact of ER-localized DENV (+) strand RNA on the translation of ER-targeted host mRNAs, the RPKM values for ER-targeted mRNAs were multiplied by corresponding ORF length, to provide a measure of gene-specific ribosome abundance (**Fig. 5C,** see also **Fig. 5D**). This transformation accounts for the fact that ribosome loading is, in general, a function of ORF length; longer ORFs tend to be more populated with ribosomes and in this scenario occupy a greater fraction of the protein translocation machinery, then shorter ORFs (61, 62). Furthermore, with prior studies demonstrating that ribosomes engaged in the translation of secretory or transmembrane proteins are bound to the Sec61 protein translocation machinery, this metric provides a measure of the fractional utilization of the ER secretory capacity by this mRNA cohort (63-65). As depicted, by 24 h post-infection, DENV (+) strand RNA occupies similar levels of ER translocon-bound ribosomes as the host ER-targeted mRNAs and by 40 h post-infection, ribosome loading onto DENV (+) strand RNA surpassed ER-targeted host mRNAs, at which point the DENV (+) strand RNA had commandeered a majority of the ER secretory capacity (**Fig. 5C**). That the sum of the ER-targeted host mRNA and DENV (+) strand RNA ribosome abundance values at 40 h exceeds the ribosome abundance of ER-targeted host mRNAs at the zero time point is consistent with the

observation that DENV infection promotes expansion of the ER compartment, as previously reported, and thus an increase in total ER translocation activity and ribosome binding capacity (66).

To further explore the impact of DENV infection on host translation, [^{35}S]Met/Cys pulse-labeling experiments were performed, again using the cell fractionation assay system depicted in **Fig. 1**. As a direct measure of *de novo* protein synthesis, [^{35}S]Met/Cys pulse-labeling provides an orthogonal test of the ribosome footprinting data and distinguishes between translating and translationally-suppressed polyribosomes, which cannot be distinguished by ribosome footprinting alone. When combined with cell fractionation, this approach also reveals differences in the translational status of the cytosol and ER compartments (44, 46). In these experiments, Huh-7 cells were infected with DENV at an MOI of 10 and pulse-labeled with [^{35}S] Met/Cys 36 h post-infection. Mock and DENV-infected cells were then fractionated and protein synthesis activity of the two compartments was assessed by phosphorimaging analysis of SDS-PAGE separated protein fractions (**Fig. 5E**). Total (unfractionated) cell extracts were obtained in parallel. As is evident in the total cell extracts, the impact of DENV infection on total proteome expression at the 36 h time point was substantial, with prominent DENV infection-dependent translation products present in the infected cells (**Fig. 5E**). The *de novo* translation patterns of the two subcellular fractions revealed distinct compartmental responses to DENV infection. Of particular interest, the overall translation pattern of the cytosol fraction at 36 h post-infection was very similar in the mock- and DENV-infected cells, with a modest suppression of overall translational activity (**Fig. 5E, Cyt Frac**) (67). Clearly evident in the cytosol fraction of the infected

348 cells was a radiolabeled band of ca. 100 kDa, which is the predicted mobility of NS5, the
349 methyltransferase-polymerase (68). Lacking transmembrane domains and/or a signal
350 peptide, NS5 would be expected to be highly enriched in the cytosol fraction, however a
351 fraction was recovered in the ER fraction as well, which may represent NS5 polymerase
352 associated with ER-bound (-) strand DENV RNA. The identity of the DENV infection-
353 specific radiolabeled band migrating slightly faster than the 100 kDa remains to be
354 determined. Contrasting with the cytosol fraction, DENV-infection elicited a dramatic
355 remodeling of the ER-associated proteome. Previously abundant ER proteins were
356 scarcely detectable and DENV proteins instead dominated the output of ER protein
357 biosynthesis (**Fig. 5E, ER Frac**). Of particular interest is the radiolabeled protein of ca.
358 68 kDa, present in the ER fraction and absent from the cytosol fraction of DENV-
359 infected cells. The mobility of this protein in SDS-PAGE is consistent with the
360 processing protease NS3. As NS3 lacks a signal sequence or transmembrane domain
361 (69), it would be predicted to reside in the cytosol. Prior studies have established that
362 NS3 associates with NS2B to form the active processing protease; with NS2B being an
363 integral membrane protein localized to the ER, this protein-protein interaction would be
364 expected to confer ER localization to soluble NS3 (68, 70, 71). To further explore these
365 findings, immunoblot analyses of DENV capsid, envelope, prM, NS2B, NS3, and NS5
366 expression and subcellular localization were performed (**Fig. 5F**). As shown, the
367 immunoblot studies were consistent with the data depicted in Fig. 5E and directly
368 demonstrate both viral protein expression and subcellular localization.

369 Combined with the ribosome footprinting data, the [^{35}S]Met/Cys pulse-labeling and
370 DENV protein immunoblot data illustrate that DENV primarily commandeers ER

translocon-associated ribosomes and suppresses translation of ER-targeted host mRNAs. Furthermore, analyses of the relative distribution of ER-bound ribosomes engaged in the translation of DENV (+) strand RNA and ER-targeted mRNAs reveal a slow process of ribosome capture by the DENV (+) strand RNA, occurring approximately in parallel with the synthesis of (+) strand DENV RNA (**Figs. 2A, 5C**).

Global translation response to DENV infection

The changes in mRNA translation patterns reported above were apparent at a transcriptomic scale. Heat map analysis of the ribosome footprinting data sets indicated a broad spectrum of altered translation by 40 h infection, though translation was largely unaffected at earlier time points when DENV (+) strand RNA levels are relatively low (**Fig. 6A**). Using a cutoff of two-fold change in total translation at the 40 h point, 948 mRNAs had enhanced translation and 880 mRNAs had suppressed translation. Importantly, the changes in translation status seen at early infection time points largely reflected lower-magnitude variants of the late infection time points. While there are specific genes that are expressed early in response to DENV infection, the majority of changes in host mRNA translation in response to DENV represent a conserved, progressive response that increases in magnitude over the time course of infection (**Fig. 6A**).

To assess the mechanisms driving these changes in gene expression, we first queried the roles of two gene expression programs known to be active during DENV infection: the interferon (IFN) pathway and the Unfolded Protein Response (UPR) (72). We defined a set of IFN-stimulated genes by treatment of Huh-7 cells with IFN-β for 12 hours. An orthologous UPR-responsive gene set was derived from a previous ribosome

profiling study that used thapsigargin treatment of mouse embryonic fibroblasts to elicit UPR activation (42). In comparing the changes in these gene sets over the course of DENV infection, each was significantly increased, indicating that the two pathways were, as expected, up-regulated (**Fig. 6B**). With regard to UPR-responsive genes, induction was quite slow and modest, more consistent with a supportive role for the UPR, e.g., expansion of ER secretory capacity, rather than an acute, proteostatic stress response (67, 73, 74). A Venn diagram of these data sets revealed a significant overlap ($p < 0.005$ for all; hypergeometic test) between genes with enhanced expression in DENV infection and both IFN induced and UPR pathways (**Fig. 6C**). However, there remained a substantial cohort of mRNAs (433) whose translation was enhanced during DENV infection, but not by IFN or UPR, which we term the DENV-only gene set (**Table S2**). These genes may represent specific host cell responses to infection or changes in gene expression driven by DENV itself. Gene ontology analysis of the 433 DENV-only genes revealed the most significant biological processes link to the GO categories autophagy, regulation of cell cycle, signal transduction, and cellular metabolism (**Fig. 6D, Table S3**).

DENV-only and IFN-induced genes differed from the rest of the transcriptome in their means of activation (**Fig. 6E**). While most transcriptome-wide changes in total translation were driven by changes in mRNA levels, changes in DENV-only genes and IFN-induced genes were primarily driven by changes in translational efficiency. The activation of the UPR was primarily transcriptional, likely through the activation of the UPR-linked transcription factors XBP-1, ATF4 and CHOP (75-77).

Given the ER-centric translational response to DENV described thus far and recent CRISPR screens for flaviviral host factors identifying primarily ER-resident proteins (27, 28), we examined how DENV infection affects the expression of high confidence DENV host factors. We focused our analysis on the Marceau, et al. (27) screen as it utilized DENV serotype 2 and Huh-7 cells, as in the current study (**Table S4**) (27). This analysis revealed many of the CRISPR-identified essential host factors to be translationally down-regulated, whereas host genes were on average unchanged (**Fig. 7A**). Specifically, of the 23 ER-resident CRISPR-identified host factor genes also present in our ribosome footprinting data set, 17 genes were translationally down-regulated at 40 h post infection ($\log_2$[40h/uninfected] < 0) and 6 were translationally up-regulated ($\log_2$[40h/uninfected] > 0), though this host factor gene set is not substantially or up- or down-regulated (**Fig. 7B**). Non-ER-resident CRISPR-identified host factors did not have a particular bias for up or down regulation (5 genes and 4 genes, respectively). The same trends in changes to translation for these CRISPR-identified host factors were seen at earlier time points, though to a lesser magnitude, as was observed with global translational changes (**Fig. 6A**). It is also of note that the changes in translation of CRISPR-identified host factors during DENV infection do not correlate with changes in their RNA levels, suggesting transcript-specific regulation of translation (**Table S1**).

Discussion

Whereas the general trajectory and biochemical machinery of DENV replication are increasingly well-understood (12, 78), major gaps in our understanding of how DENV coordinately regulates the synthesis of its RNAs and proteins remain. In addition, the fundamental question of how DENV (+) strand RNA competes for host cell translation capacity is largely unknown. Here, we mapped the landscape of transcriptional and translational responses to DENV infection in the host, and mapped the succession and subcellular organization of the RNA replication and protein synthesis events that define the DENV life cycle. DENV executes a major annexation of translation on the ER, substantially reducing the translation of most host ER-targeted mRNAs. In addition to sequestering ER-associated ribosomes, the very low translation efficiency of DENV (+) strand RNA identified here may represent a strategy for minimizing the proteostatic stress on the ER protein folding machinery, thereby limiting activation of the unfolded protein response, with its attendant PERK-mediated suppression of cap-dependent translation and general protein synthesis (79).

Combining the findings obtained in RNA-seq and Ribo-seq analysis of RNA abundance and translational status in the cytosol and ER compartments of DENV-infected human cells, a temporal order of molecular events was documented. Following viral RNA entry into the cytosol, the primary activity of DENV is (-) strand RNA synthesis. This activity, however, must be preceded by (+) strand translation for synthesis of the NS5 RNA polymerase. Once a critical concentration of DENV proteins is accumulated, the early commitment to (-) strand RNA synthesis serves as an investment that supports (+) strand replication and virion biogenesis. As infection progresses, (-) strand RNA

synthesis drops and is replaced by two primary functions: robust translation of (+) strand RNA and rapid synthesis of additional (+) strand RNA from the now-abundant (-) strand template. Following the continued buildup of DENV proteins and RNA, a population of untranslated (ribosome-free) (+) strand RNA begins to populate the cytosol, likely representing virions in the process of secretion. These data therefore reinforce the concept that the two functions of the (+) DENV RNA – a template for (-) strand synthesis and a mRNA for translation – are in direct competition, and are temporally skewed; synthesis of (-) strand RNA from the (+) strand template is prioritized through the 6 h time point, whereas translation of the (+) strand dominates thereafter.

The critical processes of DENV protein and RNA synthesis are contingent upon the virus's ability to co-opt the structure and activity of the ER. Data included here demonstrate the localization of the vast majority of the viral RNA to the ER, including the (-) strand RNA, which is untranslated and not captured in nascent viral particles. Strikingly, and as further evidence of the importance of an ER-restricted life cycle, DENV RNAs were enriched on the ER to a degree greater than host ER-targeted mRNAs (43), suggesting that there exist DENV-specific mechanisms for ensuring the highly efficient partitioning and anchoring of the (+) strand RNA to the ER. Non-structural DENV proteins, many of which are themselves integral membrane proteins, may serve important functions in this RNA anchoring process. It is also possible that DENV co-opts previously identified host cell factors that function in mRNA anchoring to the ER (40, 80, 81).

Given the intricate nature of DENV transmembrane domain synthesis and the complex polytopic topology of the polyprotein, the low translational efficiency of DENV RNA

identified here may be adaptive, as it could serve as a “kinetic trap” and thereby divert ribosomes from host mRNAs to the DENV (+) strand RNA translation. Such inefficient translation may also be adaptive from the viewpoint of ER proteostasis. Were, for example, (+) strand RNA translation to be highly efficient, the increased protein folding load on the ER would be expected to trigger activation of the UPR, leading to suppression of protein synthesis. In contrast, inefficient translation as an adaptive feature would allow for abundant (+) strand RNA for virion production while avoiding deleterious levels of UPR activation. Here we do not observe an acute or pronounced activation of the UPR, but rather a slow increase in the transcription and translation of select UPR-associated genes (**Fig. 6B and 6C**). Such a model would be consistent with earlier findings that DENV infection intersects with the UPR pathway in complex and temporally selective manner (67). The inefficiency of DENV translation likely reflects, at least in part, its highly structured 5’ UTR and a low rate of translation initiation (50, 82). These characteristics distinguish DENV (+) strand RNA from other (+) strand RNA viruses, such as the corona virus MHV, whose single stranded RNA genome is translated at an efficiency similar to host transcripts (83).

The means by which DENV controls host gene expression also reveals a highly ER-centric strategy. Over the course of DENV infection, non-DENV membrane protein synthesis is reduced at multiple levels. Thus, on the ER there is a significant reduction in the translation of these host mRNAs relative to mRNAs encoding cytosolic proteins that are also translated on ER-bound ribosomes (30, 39, 43, 84). Although there is a modest impact on host translation generally, the impact that DENV has specifically on host ER translation is large and broadly inhibitory, including a set of previously identified

503 essential host factors (discussed below). While these findings bear similarity to those
504 recently reported by Roth and coworkers (85), the two studies differ in conclusions
505 regarding the overall magnitude of the translational inhibition observed in response to
506 DENV infection. These differences likely reflect different assay systems used to asses
507 translation and in that regard we note that the magnitude of translational suppression
508 reported by Roth and coworkers via ribopuromycylation assay is similar to that reported
509 here by [^{35}S] Met/Cys incorporation and compartmental analysis of translation via Ribo-
510 seq.

511 The exceptions to the trend of suppressed translation hints at an important role for
512 translational regulation of host mRNAs by DENV itself, e.g., the enhanced translation of
513 mRNAs encoding components of the secretory pathway likely increases the cellular
514 capacity for secreting DENV virions. How this is accomplished awaits further study and
515 speaks to the emerging view of the ER as a central hub participating in the translation of
516 the mRNA transcriptome, with mRNAs localized and anchored by diverse mechanisms,
517 and the capacity for selective regulation of the translation of mRNA subsets (30).

518 The view that DENV-directed translational changes contribute to the remodeling of host
519 cell gene expression is supported by comparison of the ribosome footprinting data of
520 cells infected with DENV versus cells treated with IFN-β or thapsigargin, which activate
521 interferon response pathways or UPR, respectively. These two cellular response
522 pathways are associated with flavivirus infection and could be the driving factors for the
523 translational responses observed during DENV infection (Fig. 6). In this comparison of
524 transcriptionally activated genes, however, only subsets of IFN-activated and UPR-
525 associated genes are translationally up-regulated during DENV infection. The "DENV

only" subset of genes is generally related to regulation of catabolic processes (**Table S3**). These biological processes could ultimately favor viral replication and virion production by dedicating cellular anabolic activities toward the viral life cycle, replication of viral RNA, and folding and packaging of viral proteins. It should be considered that the specific genes found in the "DENV only" category (Table S2) may be used most directly by the virus during its lifecycle and could comprise therapeutic targets.

The high confidence links between ER physiology and the DENV viral lifecycle discussed above was also observed in recent genome-wide CRISPR screens for essential flavivirus host factors (27, 28). Interestingly, many of the identified DENV2 host factors in these past studies were found to be translationally repressed in our data sets. Though somewhat counterintuitive, this pattern may suggest a novel way of evaluating how pathogens utilize host factors. In a genetic deletion screen, as referenced here, cells experience a complete loss of gene function before they encounter a pathogen. During infection of non-genetically modified cells, however, cells are fully equipped with essential host factors at the start of infection. After the initial infection, two response branches are likely to occur: 1) cells may respond by down-regulating specific factors as a strategy to combat the infection or 2) the virus may evoke strategies to up-regulate host factors that are beneficial to its survival. As the virus has already gained access to the cell, and replication and translation have begun before the cell is able to detect and respond to the infection, the evolutionary pressure to develop a mechanism that prevents host translational repression is likely low for most genes. In this way, the virus likely allows for the translational down regulation of host factors required early in infection. It is also likely the virus has developed strategies to

upregulate specific factors that are required throughout the viral life cycle. By this logic, host factors identified by loss-of-function that are translationally repressed during infection may be therapeutically relevant targets to minimize or block initial infection, whereas host factors that are translationally activated during infection may impact viral success at later stages of infection (i.e. when an individual is already infected). This proposed bimodal evaluation of host factors, which considers not only the outcome of the virus but how the protein is regulated during infection, will require experimental validation but may provide an opportunity for insight into the questions of how and when a host factor contributes to the viral life cycle.

Cumulatively, these findings highlight the ER as not only the site of viral replication, but as an organelle that DENV dramatically remodels to fulfill the need for both biogenesis and an exit strategy from the cell. This viral habitat provides not only entry into the secretory pathway, but also a distinct environment for translational regulation that DENV controls to optimize conditions for replication (30, 86, 87). Targeting any of these points where DENV interacts with or controls the ER may be a promising area to explore anti-viral pharmaceuticals.

Materials and Methods

Cells and viruses

Huh-7 (human hepatocarcinoma cells, ATCC) were grown in 4.5g/L glucose DMEM (Gibco, USA), supplemented with 10% FBS, non-essential amino acids (Gibco, USA), 100 U/ml penicillin and 100 µg/ml streptomycin (Gibco, USA). Cells were cultured at 37°C in a humidified 5% CO_2 incubator. DENV strain DENV2-NGC (GenBank accession M29095.1) was used for experiments. Viruses were grown in C6/36 cells and titered by standard Vero foci forming assay.

Viral infection protocol

Huh-7 cells were plated at a density of $2x10^6$ cells per $10cm^2$ dish. Cells were infected with DENV-2 NGC strain at a MOI (multiplicity of infection) of 10 for 1h, the virus inoculums were then removed and cells washed once with PBS before replacing with pre-warmed complete media. MOIs were calculated using Vero cell-based titers as noted above. Interferon treatment was performed using recombinant Interferon beta 1A (Millipore) for 12 hours at 500 units/mL.

Cell fractionation

Cells were treated with 180µM cycloheximide for 30 seconds then washed with cold PBS. Cells were then separated into their cytosolic and ER compartments as previously described (39, 43, 45, 84, 88, 89). Briefly, the cytosol fraction was extracted by addition of a buffer containing 0.03% digitonin, 110 mM KOAc, 25 mM K-HEPES pH 7.2, 15 mM $MgCl_2$, and 4 mM $CaCl_2$ to the dish and incubated in ice for 5 min. The buffer was collected, and cells washed with the same buffer containing 0.0015% digitonin. The first lysis and the wash were combined and represent the cytosolic contents of the cell. The

ER fraction was then collected by lysis of the digitonin-extracted cells with an ER lysis buffer containing 2% n-dodecyl-β-D-maltoside, 200 mM KOAc, 25 mM K-HEPES pH 7.2, 15 mM MgCl2, and 4 mM $CaCl_2$.

Ribosome profiling and RNA-seq

Cell lysates were diluted to 100 mM KOAc and treated with 10 µg/mL micrococcal nuclease for 30 min at 37°C. Ribosomes were pelleted by ultracentrifugation through a 0.5M sucrose cushion in a Beckman TL100 ultracentrifuge, using the TLA100.2 rotor (24 min, 90,000 RPM). Ribosomal pellets were subjected to phenol/chloroform extraction, the RNA isolated, and subsequently treated with polynucleotide kinase (New England Biolabs). Ribosome-protected mRNA fragments were then size-selected by acrylamide gel electrophoresis, extracted, and assembled into cDNA libraries as described in previous publications from this lab and summarized below (42, 90).

For mRNA-seq, total RNA was isolated from lysates by phenol/chloroform extraction. rRNA was depleted using RiboZero (Illumina). Eluted mRNA was fragmented by resuspending in 100 µL 40 mM Tris-OAc pH 8.3, 100 mM KOAc 30 mM MgOAc and heating to 95°C for 10 min. Fragmented RNA was precipitated by addition of NaOAC to 300 mM and 300 µL ethanol, the solution chilled on ice, and RNA collected by centrifugation. The RNA pellet was resuspended in a 10 µL solution containing 10 mM ATP, 10 U polynucleotide kinase (New England Biolabs), and 1 X PNK buffer. This solution was incubated at 37 °C for 30 minutes, then heat inactivated at 95 °C for 10 min.

610 Each of the RNA fragment pools was converted into a cDNA library using the NEBNext
611 Small RNA Library Prep Set for Illumina (New England Biolabs) as described by the
612 manufacturer, except using half reactions. cDNA libraries were amplified using 16
613 cycles of PCR, then pooled and sequenced using the HiSeq 2500 (Illumina). Reads are
614 available under Gene Expression Omnibus Accession GSE69602.

615 **Analysis of protein and RNA compositions of subcellular fractions.**

616 Huh-7 cells were mock-infected or DENV-infected (MOI = 10) and fractionated into
617 cytosol and endoplasmic reticulum (ER) fractions as described above. Fractions were
618 either subjected to tricholoracetic acid precipitation, to recover the protein fraction, or
619 extracted with Trizol® to obtain the total RNA fraction. To analyze protein distributions in
620 the two subfractions, samples were resuspended in SDS-PAGE sample buffer,
621 separated on 12.5% SDS-PAGE gels, transferred to nitrocellulose membranes and
622 protein distributions analyzed by immunoblot using the following monoclonal antibodies
623 GAPDH: DSHB-hGAPDH-2G7; tubulin: 6G7; and rabbit polyclonal antisera recognizing
624 ribophorin I and TRAPα. Monoclonal antibodies were obtained from the Developmental
625 Studies Hybridoma Bank, created by the NICHD of the NIH and maintained at The
626 University of Iowa, Department of Biology, Iowa City, IA 52242. Rabbit antisera were
627 generated by immunization with KLH-synthetic peptide conjugates and were
628 characterized in prior reports from the Nicchitta laboratory (39, 41, 88). For analysis of
629 viral protein expression, Huh7 cells were plated at 3 x 10^5 cells in a six-well dish and
630 infected the following day with DENV-2 (NGC) MOI of 10, as described above. Infection
631 was allowed to carry on for 36 h and then cells were fractionated into cytoplasmic and
632 ER fractions as described above. Proteins were TCA precipitated and re-suspended in

633 1x LDS loading buffer (Novex). Proteins were heated at 95˚C for 5 minutes, and the
634 same volume of lysate for each compartment was separated on a 4-12% SDS-PAGE
635 gel (Novex), the proteins transferred to nitrocellulose membranes, and expressed
636 proteins detected using antibodies against C, prM, E, NS1, NS2B, NS4B, NS3 or NS5
637 (Genetex) and fluorescence-based detection (LI-COR).

638 To assess RNA compositions, samples were separated on agarose gels, stained with
639 SYBR® Green II, and imaged on a GE Healthcare Amersham Imager 600.

640 **Metabolic labeling of tissue culture cells**

641 Huh-7 cells were plated at $3x10^6$ cells per well in a six-well dish and infected as above.
642 At the end of infections, cells were incubated in methionine and cysteine free media for
643 30 minutes to deplete internal pools of these amino acids. Cells were then labeled by
644 addition of 0.2 mCi/mL [^{35}S]Met/Cys media for 30 minutes, washed with PBS three
645 times, and lysed with a buffer consisting of 400 mM KOAc, 15mM Mg(OAc)2, 25 mM
646 HEPES, pH 7.6, 1% NP-40, and 1 mM DTT. Proteins were TCA precipitated and
647 resuspended in 1x LDS loading buffer (Novex). Proteins were separated on a 4-12%
648 acrylamide gel (Novex), dried, and the gels were phosphorimaged using a GE Typhoon
649 Trio.

650 **Data analysis**

651 Reads were first trimmed of their 3' adapters using Cutadapt (91). A reference
652 transcriptome was generated with Tophat and Cufflinks (92), using combined RNA-seq
653 data to generate a consensus transcriptome from Refseq release 68. The most
654 abundant isoform of each gene was selected and compiled into a reference

transcriptome. All reads were then mapped using Bowtie (93), allowing no mismatches. Reads within the coding sequence were counted and normalized by coding sequence length and library size to give total translation and mRNA counts. Genes where fewer than 4 reads were mapped were discarded for that sample. sfRNA levels were determined via the equation (3' UTR read density/CDS read density) x RPKM (DENV CDS).

To calculate the rates of change in DENV RNA levels, changes in RNA levels were fitted to an exponential growth model $y_{t+1} = y_t \times e^{k\Delta t}$, where y is the RNA level time *t* and *k* is the growth rate. This equation was solved for *k* and converted to a percentage: $k = 100 \times \ln\left(\frac{y_{t+1}}{y_t}\right) / \Delta t$.

Relative contributions of mRNA levels and ribosome loading to overall changes in ribosome footprinting data were performed as described in (94), where the percentage of change driven by mRNA levels is calculated by the geometric mean of correlations between RNA-seq fold changes and ribosome footprinting fold changes, divided by the correlations between ribosome footprinting replicates. Changes in ribosome loading are inferred to contribute the remainder of the fold change.

All sequencing data are available at GEO accession number GSE69602.

Acknowledgements

We thank the members of the Nicchitta, Garcia-Blanco, and Vasudevan labs, as well as Shirish Shenolikar at Duke-NUS Medical School, for providing an energizing intellectual environment and critical feedback on the manuscript. This work was supported through Duke/Duke-NUS Research Collaboration Awards 2014/0013 and 2016/0025 (CVN and SGV), NMRC/MOHIAFCat1/0018/2014 (SGV), NIH RO1AI089526 and RO1AI101431 (MAGB), and NIH GM101533-05A1 and NIH GM118630-01A1 (CVN). We thank Shirish Shenolikar, Duke-NUS, for partial funding of salary support for DR and the National Science Foundation Graduate Research Fellowship Program Grant No. DGS-1644868 for funding tuition and stipend for JC. The funders had no role in study design, data collection and analysis, decision to publish, or preparation of the manuscript. Any opinions, findings, and conclusions or recommendations expressed in this material are those of the author(s) and do not necessarily reflect the views of the National Science Foundation.

References

1. **Gingras AC, Svitkin Y, Belsham GJ, Pause A, Sonenberg N.** 1996. Activation of the translational suppressor 4E-BP1 following infection with encephalomyocarditis virus and poliovirus. Proceedings of the National Academy of Sciences of the United States of America **93:**5578-5583.
2. **Borman AM, Michel YM, Kean KM.** 2001. Detailed analysis of the requirements of hepatitis A virus internal ribosome entry segment for the eukaryotic initiation factor complex eIF4F. Journal of virology **75:**7864-7871.
3. **Kuyumcu-Martinez M, Belliot G, Sosnovtsev SV, Chang KO, Green KY, Lloyd RE.** 2004. Calicivirus 3C-like proteinase inhibits cellular translation by cleavage of poly(A)-binding protein. Journal of virology **78:**8172-8182.
4. **Komarova AV, Real E, Borman AM, Brocard M, England P, Tordo N, Hershey JW, Kean KM, Jacob Y.** 2007. Rabies virus matrix protein interplay with eIF3, new insights into rabies virus pathogenesis. Nucleic acids research **35:**1522-1532.
5. **He B, Gross M, Roizman B.** 1997. The gamma(1)34.5 protein of herpes simplex virus 1 complexes with protein phosphatase 1alpha to dephosphorylate the alpha subunit of the eukaryotic translation initiation factor 2 and preclude the shutoff of protein synthesis by double-stranded RNA-activated protein kinase. Proceedings of the National Academy of Sciences of the United States of America **94:**843-848.
6. **Aoyagi M, Gaspar M, Shenk TE.** 2010. Human cytomegalovirus UL69 protein facilitates translation by associating with the mRNA cap-binding complex and excluding 4EBP1. Proceedings of the National Academy of Sciences of the United States of America **107:**2640-2645.
7. **Abernathy E, Gilbertson S, Alla R, Glaunsinger B.** 2015. Viral Nucleases Induce an mRNA Degradation-Transcription Feedback Loop in Mammalian Cells. Cell host & microbe **18:**243-253.
8. **Walsh D, Mathews MB, Mohr I.** 2013. Tinkering with translation: protein synthesis in virus-infected cells. Cold Spring Harbor perspectives in biology **5:**a012351.
9. **Leong K, Lee W, Berk AJ.** 1990. High-level transcription from the adenovirus major late promoter requires downstream binding sites for late-phase-specific factors. Journal of virology **64:**51-60.
10. **Guarino LA, Summers MD.** 1986. Interspersed Homologous DNA of Autographa californica Nuclear Polyhedrosis Virus Enhances Delayed-Early Gene Expression. Journal of virology **60:**215-223.
11. **Walsh D, Mohr I.** 2011. Viral subversion of the host protein synthesis machinery. Nature reviews Microbiology **9:**860-875.
12. **Paranjape SM, Harris E.** 2010. Control of dengue virus translation and replication. Curr Top Microbiol Immunol **338:**15-34.
13. **Screaton G, Mongkolsapaya J, Yacoub S, Roberts C.** 2015. New insights into the immunopathology and control of dengue virus infection. Nat Rev Immunol **15:**745-759.

14. **Diamond MS, Pierson TC.** 2015. Molecular Insight into Dengue Virus Pathogenesis and Its Implications for Disease Control. Cell **162:**488-492.
15. **Edgil D, Polacek C, Harris E.** 2006. Dengue virus utilizes a novel strategy for translation initiation when cap-dependent translation is inhibited. J Virol **80:**2976-2986.
16. **Pena J, Harris E.** 2011. Dengue virus modulates the unfolded protein response in a time-dependent manner. J Biol Chem **286:**14226-14236.
17. **Dong H, Fink K, Zust R, Lim SP, Qin CF, Shi PY.** 2014. Flavivirus RNA methylation. J Gen Virol **95:**763-778.
18. **Mukhopadhyay S, Kuhn RJ, Rossmann MG.** 2005. A structural perspective of the flavivirus life cycle. Nat Rev Microbiol **3:**13-22.
19. **Cologna R, Rico-Hesse R.** 2003. American genotype structures decrease dengue virus output from human monocytes and dendritic cells. J Virol **77:**3929-3938.
20. **Klema VJ, Padmanabhan R, Choi KH.** 2015. Flaviviral Replication Complex: Coordination between RNA Synthesis and 51-RNA Capping. Viruses **7:**4640-4656.
21. **Gamarnik AV, Andino R.** 1998. Switch from translation to RNA replication in a positive-stranded RNA virus. Genes & development **12:**2293-2304.
22. **Villordo SM, Filomatori CV, Sanchez-Vargas I, Blair CD, Gamarnik AV.** 2015. Dengue virus RNA structure specialization facilitates host adaptation. PLoS pathogens **11:**e1004604.
23. **Villordo SM, Alvarez DE, Gamarnik AV.** 2010. A balance between circular and linear forms of the dengue virus genome is crucial for viral replication. RNA **16:**2325-2335.
24. **Stohlman SA, Wisseman CL, Jr., Eylar OR, Silverman DJ.** 1975. Dengue virus-induced modifications of host cell membranes. J Virol **16:**1017-1026.
25. **Miller S, Sparacio S, Bartenschlager R.** 2006. Subcellular localization and membrane topology of the Dengue virus type 2 Non-structural protein 4B. J Biol Chem **281:**8854-8863.
26. **Heaton NS, Mosca F, Fenouil R, Gardner TJ, Aguirre S, Shah PS, Zhou N, Manganaro L, Hultquist JF, Noel J, Sachs DH, Hamilton J, Leon PE, Chawdury A, Tripathi S, Melegari C, Campisi L, Hai R, Meteveli G, Gamarnik AV, Garcia-Sastre A, Greenbaum B, Simon V, Fernandez-Sesma A, Krogan NJ, Mulder LC, van Bakel H, Tortorella D, Taunton J, Palese P, Marazzi I.** 2016. Targeting Viral Proteostasis Limits Influenza Virus, HIV, and Dengue Virus Infection. Immunity **44:**46-58.
27. **Marceau CD, Puschnik AS, Majzoub K, Ooi YS, Brewer SM, Fuchs G, Swaminathan K, Mata MA, Elias JE, Sarnow P, Carette JE.** 2016. Genetic dissection of Flaviviridae host factors through genome-scale CRISPR screens. Nature **535:**159-163.
28. **Zhang R, Miner JJ, Gorman MJ, Rausch K, Ramage H, White JP, Zuiani A, Zhang P, Fernandez E, Zhang Q, Dowd KA, Pierson TC, Cherry S, Diamond MS.** 2016. A CRISPR screen defines a signal peptide processing pathway required by flaviviruses. Nature **535:**164-168.

29. **Staudacher JJ, Naarmann-de Vries IS, Ujvari SJ, Klinger B, Kasim M, Benko E, Ostareck-Lederer A, Ostareck DH, Bondke Persson A, Lorenzen S, Meier JC, Bluthgen N, Persson PB, Henrion-Caude A, Mrowka R, Fahling M.** 2015. Hypoxia-induced gene expression results from selective mRNA partitioning to the endoplasmic reticulum. Nucleic acids research **43:**3219-3236.
30. **Reid DW, Nicchitta CV.** 2015. Diversity and selectivity in mRNA translation on the endoplasmic reticulum. Nat Rev Mol Cell Biol **16:**221-231.
31. **Reid DW, Nicchitta CV.** 2012. Primary Role for Endoplasmic Reticulum-bound Ribosomes in Cellular Translation Identified by Ribosome Profiling. The Journal of Biological Chemistry **287:**5518-5527.
32. **Stephens SB, Nicchitta CV.** 2008. Divergent regulation of protein synthesis in the cytosol and endoplasmic reticulum compartments of mammalian cells. Molecular biology of the cell **19:**623-632.
33. **Diehn M, Eisen MB, Botstein D, Brown PO.** 2000. Large-scale identification of secreted and membrane-associated gene products using DNA microarrays. Nature genetics **25:**58-62.
34. **Ingolia NT.** 2014. Ribosome profiling: new views of translation, from single codons to genome scale. Nat Rev Genet **15:**205-213.
35. **Ingolia NT, Ghaemmaghami S, Newman JR, Weissman JS.** 2009. Genome-wide analysis in vivo of translation with nucleotide resolution using ribosome profiling. Science **324:**218-223.
36. **Jagannathan S, Nwosu C, Nicchitta CV.** 2011. Analyzing mRNA localization to the endoplasmic reticulum via cell fractionation. Methods in molecular biology **714:**301-321.
37. **Inoue T, Tsai B.** 2013. How viruses use the endoplasmic reticulum for entry, replication, and assembly. Cold Spring Harb Perspect Biol **5:**a013250.
38. **Welsch S, Miller S, Romero-Brey I, Merz A, Bleck CK, Walther P, Fuller SD, Antony C, Krijnse-Locker J, Bartenschlager R.** 2009. Composition and three-dimensional architecture of the dengue virus replication and assembly sites. Cell Host Microbe **5:**365-375.
39. **Lerner RS, Seiser RM, Zheng T, Lager PJ, Reedy MC, Keene JD, Nicchitta CV.** 2003. Partitioning and translation of mRNAs encoding soluble proteins on membrane-bound ribosomes. RNA **9:**1123-1137.
40. **Jagannathan S, Hsu JC, Reid DW, Chen Q, Thompson WJ, Moseley AM, Nicchitta CV.** 2014. Multifunctional roles for the protein translocation machinery in RNA anchoring to the endoplasmic reticulum. The Journal of biological chemistry **289:**25907-25924.
41. **Jagannathan S, Nwosu C, Nicchitta CV.** 2011. Analyzing mRNA localization to the endoplasmic reticulum via cell fractionation. Methods Mol Biol **714:**301-321.
42. **Reid DW, Chen Q, Tay AS, Shenolikar S, Nicchitta CV.** 2014. The unfolded protein response triggers selective mRNA release from the endoplasmic reticulum. Cell **158:**1362-1374.
43. **Reid DW, Nicchitta CV.** 2012. Primary role for endoplasmic reticulum-bound ribosomes in cellular translation identified by ribosome profiling. J Biol Chem **287:**5518-5527.

44. **Stephens SB, Dodd RD, Brewer JW, Lager PJ, Keene JD, Nicchitta CV.** 2005. Stable ribosome binding to the endoplasmic reticulum enables compartment-specific regulation of mRNA translation. Mol Biol Cell **16:**5819-5831.

45. **Stephens SB, Dodd RD, Lerner RS, Pyhtila BM, Nicchitta CV.** 2008. Analysis of mRNA partitioning between the cytosol and endoplasmic reticulum compartments of mammalian cells. Methods Mol Biol **419:**197-214.

46. **Stephens SB, Nicchitta CV.** 2008. Divergent regulation of protein synthesis in the cytosol and endoplasmic reticulum compartments of mammalian cells. Mol Biol Cell **19:**623-632.

47. **Junjhon J, Lausumpao M, Supasa S, Noisakran S, Songjaeng A, Saraithong P, Chaichoun K, Utaipat U, Keelapang P, Kanjanahaluethai A, Puttikhunt C, Kasinrerk W, Malasit P, Sittisombut N.** 2008. Differential modulation of prM cleavage, extracellular particle distribution, and virus infectivity by conserved residues at nonfurin consensus positions of the dengue virus pr-M junction. Journal of virology **82:**10776-10791.

48. **Liu ZY, Li XF, Jiang T, Deng YQ, Ye Q, Zhao H, Yu JY, Qin CF.** 2016. Viral RNA switch mediates the dynamic control of flavivirus replicase recruitment by genome cyclization. Elife **5.**

49. **Araujo PR, Yoon K, Ko D, Smith AD, Qiao M, Suresh U, Burns SC, Penalva LO.** 2012. Before It Gets Started: Regulating Translation at the 5' UTR. Comp Funct Genomics **2012:**475731.

50. **Gebhard LG, Filomatori CV, Gamarnik AV.** 2011. Functional RNA elements in the dengue virus genome. Viruses **3:**1739-1756.

51. **Iglesias NG, Gamarnik AV.** 2011. Dynamic RNA structures in the dengue virus genome. RNA Biol **8:**249-257.

52. **Irigoyen N, Firth AE, Jones JD, Chung BY, Siddell SG, Brierley I.** 2016. High-Resolution Analysis of Coronavirus Gene Expression by RNA Sequencing and Ribosome Profiling. PLoS pathogens **12:**e1005473.

53. **Firth AE, Blitvich BJ, Wills NM, Miller CL, Atkins JF.** 2010. Evidence for ribosomal frameshifting and a novel overlapping gene in the genomes of insect-specific flaviviruses. Virology **399:**153-166.

54. **Firth AE, Brierley I.** 2012. Non-canonical translation in RNA viruses. J Gen Virol **93:**1385-1409.

55. **Markoff L.** 1989. In vitro processing of dengue virus structural proteins: cleavage of the pre-membrane protein. Journal of virology **63:**3345-3352.

56. **Clum S, Ebner KE, Padmanabhan R.** 1997. Cotranslational membrane insertion of the serine proteinase precursor NS2B-NS3(Pro) of dengue virus type 2 is required for efficient in vitro processing and is mediated through the hydrophobic regions of NS2B. The Journal of biological chemistry **272:**30715-30723.

57. **Pijlman GP, Funk A, Kondratieva N, Leung J, Torres S, van der Aa L, Liu WJ, Palmenberg AC, Shi PY, Hall RA, Khromykh AA.** 2008. A highly structured, nuclease-resistant, noncoding RNA produced by flaviviruses is required for pathogenicity. Cell host & microbe **4:**579-591.

58. **Manokaran G, Finol E, Wang C, Gunaratne J, Bahl J, Ong EZ, Tan HC, Sessions OM, Ward AM, Gubler DJ, Harris E, Garcia-Blanco MA, Ooi EE.** 2015. Dengue subgenomic RNA binds TRIM25 to inhibit interferon expression for epidemiological fitness. Science **350:**217-221.

59. **Pyhtila B, Zheng T, Lager PJ, Keene JD, Reedy MC, Nicchitta CV.** 2008. Signal sequence- and translation-independent mRNA localization to the endoplasmic reticulum. RNA **14:**445-453.

60. **Diehn M, Bhattacharya R, Botstein D, Brown PO.** 2006. Genome-scale identification of membrane-associated human mRNAs. PLoS genetics **2:**e11.

61. **Arava Y, Boas FE, Brown PO, Herschlag D.** 2005. Dissecting eukaryotic translation and its control by ribosome density mapping. Nucleic Acids Res **33:**2421-2432.

62. **Rogers DW, Bottcher MA, Traulsen A, Greig D.** 2017. Ribosome reinitiation can explain length-dependent translation of messenger RNA. PLoS Comput Biol **13:**e1005592.

63. **Beckmann R, Spahn CM, Frank J, Blobel G.** 2001. The active 80S ribosome-Sec61 complex. Cold Spring Harb Symp Quant Biol **66:**543-554.

64. **Menetret JF, Hegde RS, Aguiar M, Gygi SP, Park E, Rapoport TA, Akey CW.** 2008. Single copies of Sec61 and TRAP associate with a nontranslating mammalian ribosome. Structure **16:**1126-1137.

65. **Voorhees RM, Fernandez IS, Scheres SH, Hegde RS.** 2014. Structure of the mammalian ribosome-Sec61 complex to 3.4 A resolution. Cell **157:**1632-1643.

66. **Pena J, Harris E.** 2012. Early dengue virus protein synthesis induces extensive rearrangement of the endoplasmic reticulum independent of the UPR and SREBP-2 pathway. PLoS One **7:**e38202.

67. **Pena J, Harris E.** 2011. Dengue virus modulates the unfolded protein response in a time-dependent manner. The Journal of biological chemistry **286:**14226-14236.

68. **Perera R, Kuhn RJ.** 2008. Structural proteomics of dengue virus. Curr Opin Microbiol **11:**369-377.

69. **Luo D, Xu T, Hunke C, Gruber G, Vasudevan SG, Lescar J.** 2008. Crystal structure of the NS3 protease-helicase from dengue virus. J Virol **82:**173-183.

70. **Chambers TJ, Nestorowicz A, Amberg SM, Rice CM.** 1993. Mutagenesis of the yellow fever virus NS2B protein: effects on proteolytic processing, NS2B-NS3 complex formation, and viral replication. J Virol **67:**6797-6807.

71. **Falgout B, Pethel M, Zhang YM, Lai CJ.** 1991. Both nonstructural proteins NS2B and NS3 are required for the proteolytic processing of dengue virus nonstructural proteins. J Virol **65:**2467-2475.

72. **Umareddy I, Pluquet O, Wang QY, Vasudevan SG, Chevet E, Gu F.** 2007. Dengue virus serotype infection specifies the activation of the unfolded protein response. Virology Journal **4:**91.

73. **Walter P, Ron D.** 2011. The unfolded protein response: from stress pathway to homeostatic regulation. Science **334:**1081-1086.

74. **Iwakoshi NN, Lee AH, Vallabhajosyula P, Otipoby KL, Rajewsky K, Glimcher LH.** 2003. Plasma cell differentiation and the unfolded protein response intersect at the transcription factor XBP-1. Nat Immunol **4.**

75. **Han J, Kaufman RJ.** 2017. Physiological/pathological ramifications of transcription factors in the unfolded protein response. Genes Dev **31:**1417-1438.
76. **Ron D, Walter P.** 2007. Signal integration in the endoplasmic reticulum unfolded protein response. Nat Rev Mol Cell Biol **8:**519-529.
77. **Schroder M, Kaufman RJ.** 2005. The mammalian unfolded protein response. Annu Rev Biochem **74:**739-789.
78. **Bidet K, Garcia-Blanco MA.** 2014. Flaviviral RNAs: weapons and targets in the war between virus and host. The Biochemical journal **462:**215-230.
79. **Ron D, Walter P.** 2007. Signal integration in the endoplasmic reticulum unfolded protein response. Nature reviews Molecular cell biology **8:**519-529.
80. **Chen Q, Jagannathan S, Reid DW, Zheng T, Nicchitta CV.** 2011. Hierarchical regulation of mRNA partitioning between the cytoplasm and the endoplasmic reticulum of mammalian cells. Molecular Biology of the Cell **22:**2646-2658.
81. **Cui XA, Palazzo AF.** 2014. Localization of mRNAs to the endoplasmic reticulum. Wiley interdisciplinary reviews RNA doi:10.1002/wrna.1225.
82. **Iglesias NG, Gamarnik AV.** 2011. Dynamic RNA structures in the dengue virus genome. RNA biology **8:**249-257.
83. **Irigoyen N, Firth AE, Jones JD, Chung BY, Siddell SG, Brierley I.** 2016. High-Resolution Analysis of Coronavirus Gene Expression by RNA Sequencing and Ribosome Profiling. PLoS Pathog **12:**e1005473.
84. **Lerner RS, Nicchitta CV.** 2006. mRNA translation is compartmentalized to the endoplasmic reticulum following physiological inhibition of cap-dependent translation. RNA **12:**775-789.
85. **Roth H, Magg V, Uch F, Mutz P, Klein P, Haneke K, Lohmann V, Bartenschlager R, Fackler OT, Locker N, Stoecklin G, Ruggieri A.** 2017. Flavivirus Infection Uncouples Translation Suppression from Cellular Stress Responses. MBio **8**.
86. **Li S, Liu L, Zhuang X, Yu Y, Liu X, Cui X, Ji L, Pan Z, Cao X, Mo B, Zhang F, Raikhel N, Jiang L, Chen X.** 2013. MicroRNAs inhibit the translation of target mRNAs on the endoplasmic reticulum in Arabidopsis. Cell **153:**562-574.
87. **Stalder L, Heusermann W, Sokol L, Trojer D, Wirz J, Hean J, Fritzsche A, Aeschimann F, Pfanzagl V, Basselet P, Weiler J, Hintersteiner M, Morrissey DV, Meisner-Kober NC.** 2013. The rough endoplasmatic reticulum is a central nucleation site of siRNA-mediated RNA silencing. EMBO J **32:**1115-1127.
88. **Jagannathan S, Hsu JC, Reid DW, Chen Q, Thompson WJ, Moseley AM, Nicchitta CV.** 2014. Multifunctional roles for the protein translocation machinery in RNA anchoring to the endoplasmic reticulum. J Biol Chem **289:**25907-25924.
89. **Stephens SB, Nicchitta CV.** 2007. In vitro and tissue culture methods for analysis of translation initiation on the endoplasmic reticulum. Methods Enzymol **431:**47-60.
90. **Reid DW, Shenolikar S, Nicchitta CV.** 2015. Simple and inexpensive ribosome profiling analysis of mRNA translation. Methods doi:10.1016/j.ymeth.2015.07.003.
91. **Martin M.** 2011. Cutadapt removes adapter sequences from high-throughput sequencing reads. EMBnetjournal **17:**10-12.

92. **Pollier J, Rombauts S, Goossens A.** 2013. Analysis of RNA-Seq data with TopHat and Cufflinks for genome-wide expression analysis of jasmonate-treated plants and plant cultures. Methods Mol Biol **1011:**305-315.

93. **Langmead B, Trapnell C, Pop M, Salzberg SL.** 2009. Ultrafast and memory-efficient alignment of short DNA sequences to the human genome. Genome biology **10:**R25.

94. **Jovanovic M, Rooney MS, Mertins P, Przybylski D, Chevrier N, Satija R, Rodriguez EH, Fields AP, Schwartz S, Raychowdhury R, Mumbach MR, Eisenhaure T, Rabani M, Gennert D, Lu D, Delorey T, Weissman JS, Carr SA, Hacohen N, Regev A.** 2015. Immunogenetics. Dynamic profiling of the protein life cycle in response to pathogens. Science **347:**1259038.

Figure Legends

Figure 1. Experimental schematic and validation of cell fractionation protocol. A) Schematic of the experimental approach. Mock- or DEV-infected Huh7 cells were fractionated by a sequential detergent extraction protocol where cell cultures are first treated with digitonin-supplemented buffers to release the cytosolic contents followed by a subsequent treatment with dodecylmaltoside (DDM)-supplemented buffers to release the ER-associated contents. Total RNA was isolated from each fraction and analyzed by RNA-Seq to assess gene expression. In parallel, polysomes in each fraction were nuclease digested, ribosome footprints isolated, and analyzed by Ribo-Seq. **B)** Immunoblot analysis of the distributions of cytosolic (GAPDH and tubulin) and ER resident membrane (Ribophorin I and TRAPα) proteins in the cytosol (Cyt) and ER fractions of mock-infected cells and following 40 h of DENV infection (MOI = 10). **C)** Ribosome and tRNA distributions in the two subcellular fractions were determined by isolation of total RNA, separation by agarose gel electrophoresis, and visualization with SYBR Green staining. 18S, 28S and tRNA components are indicated.

Figure 2. Spatiotemporal organization of DENV replication and translation. A) Abundance of DENV (+) and (-) RNA over a 40 h infection time course, as assessed by RNA-seq. **B)** Rate of accumulation for DENV (+) and (-) RNA. Each point indicates the average rate of change of RNA abundance between the two adjacent time points, expressed as percent change per hour in an exponential growth model. **C)** Percentage of DENV + strand RNA, - strand RNA, and + strand translation that is ER-associated throughout the experimental time course. **D)** Translational efficiency of DENV RNA

relative to the host transcriptome. The translation efficiency distributions of host mRNAs encoding TMHMM-predicted ER-targeted proteins is shown in black, with the translation efficiency of DENV RNA in red. The translation efficiency distribution is calculated as an average value of all mRNAs at all time points. For all panels, error bars represent ±SD (n=2).

Figure 3. Ribosome footprinting pattern of the DENV RNA. A) Ribosome density across the DENV RNA at each infection time point as a 30-nt moving window. Red lines separate different coding sequences, while the grey area indicates the entire polyprotein coding sequence. **B)** Schematic representation of the DENV polyprotein with each protein color-coded as legend for panel **C**. **C)** Ribosome density for each viral protein coding region over the course of infection (color legend, panel **B**).

Figure 4. sfRNA abundance and subcellular localization. A) RNA-seq read density in the cytosol and ER fractions along the DENV RNA sequence. The coding sequence is indicated by the grey shaded area and different coding sequences by red lines. The sfRNA is derived from the DENV 3' UTR. **B)** Subcellular localization of the sfRNA relative to the (+) strand DENV RNA. **C)** Distribution of read lengths for ribosome profiling reads mapping to the transcriptome, DENV coding sequence, and DENV 3' UTR.

Figure 5. DENV selectively remodels the ER translational landscape. A) Change in the total translation of mRNAs over the infection time course, as assessed by ribosome footprinting. Two categories of mRNAs are plotted: mRNAs encoding ER-targeted proteins, which encode a signal sequence or transmembrane domain, and mRNAs

encoding cytosolic proteins, which do not. Total translation was measured as the total number of ribosome footprinting reads mapped to an mRNA cohort, normalized for library size, and then expressed as a percentage of that value in mock infected cells. DENV RNAs were excluded from these calculations. **B)** As in A, except mRNA levels are depicted, as measured by RNA-seq and normalized to length. **C)** Time course of ribosome recruitment by ER-associated DENV (+) RNA. Illustrated is the fractional capture of ER-bound ribosomes translating topogenic signal-encoding mRNAs (signal sequence and/or transmembrane domains, i.e. ER-targeted host mRNA) and DENV (+) RNA, as determined from the Ribo-seq datasets. Ribosome abundance is calculated as RPKM x CDS length x 10^6. **D)** Fraction of ER-bound ribosomes translating non-topogenic signal-encoding mRNAs (i.e. cytosol-encoding host mRNA) and DENV (+) RNA, as calculated in **4C**. **E)** Metabolic labeling of newly-synthesized total, ER-associated and cytosolic proteins. Cells were infected with DENV for 36 h then pulse-labeled with [^{35}S]Met/Cys. Cells were either directly detergent extracted (Total) or fractionated as in illustrated in Fig.1 to obtain ER and cytosol (Cyt) fractions and analyzed by SDS-PAGE followed by autoradiography. Bands appearing samples from the DENV infected samples are presumed to be DENV proteins and are labeled based on known molecular weight. **F)** Immunoblot analyses of a subset of DENV proteins confirms expression and subcellular distributions indicated in panel E.

Figure 6. Host gene expression response to DENV infection. **A)** Heat map of changes in total translation of host genes over the DENV infection time course. Genes are sorted by their mean response over the time course of infection. The translational

response to interferon beta 1A treatment is also indicated. **B)** Changes during DENV infection in the interferon-induced-only gene set (defined as those genes increased at least 50% after treatment with interferon beta 1A) and the UPR-induced gene set (genes increased at least 50% after 4 h UPR induction)(UPR gene set from (42)). **C)** Venn diagram specifying the overlaps between the interferon and UPR gene sets described above and the genes increased at least 100% in total translation after 40 h DENV infection. **D)** Five most significant gene ontology terms for DENV-only gene set determined for biological process using GOrilla with the full data set as the background list. **E)** The contributions of changes in mRNA levels and translational efficiency to changes in total translational activity after 40 h DENV infection. These values were calculated as described in Materials and Methods for all genes and for each set of genes that is exclusively identified as DENV, UPR, or IFN.

Figure 7. Translational changes of CRISPR-identified host factors during DENV infection. A) Histogram showing changes in total translation for CRISPR-identified essential genes for DENV2 as determined in Marceau, et al. (27). Genes that were essential for DENV replication and with a RIGER score of > 1 were operationally scored as essential, while all other genes were scored as non-essential. **B)** List of $\log_2$ change in translation for CRISPR-identified essential genes for DENV2 as determined in Marceau, et al. (27), with RIGER score of > 1, after 40 h infection. These values were calculated as described in Materials and Methods. The ER-localization status of each gene product is also indicated.

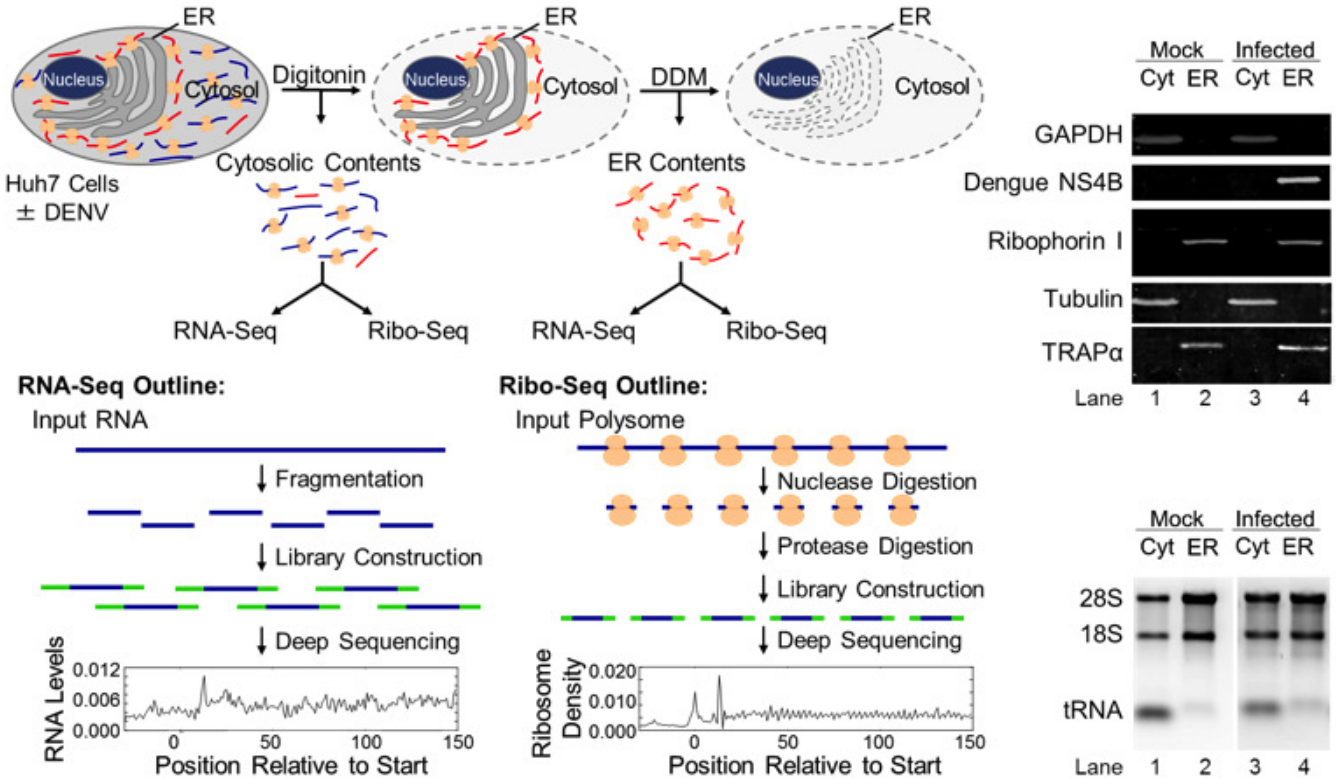

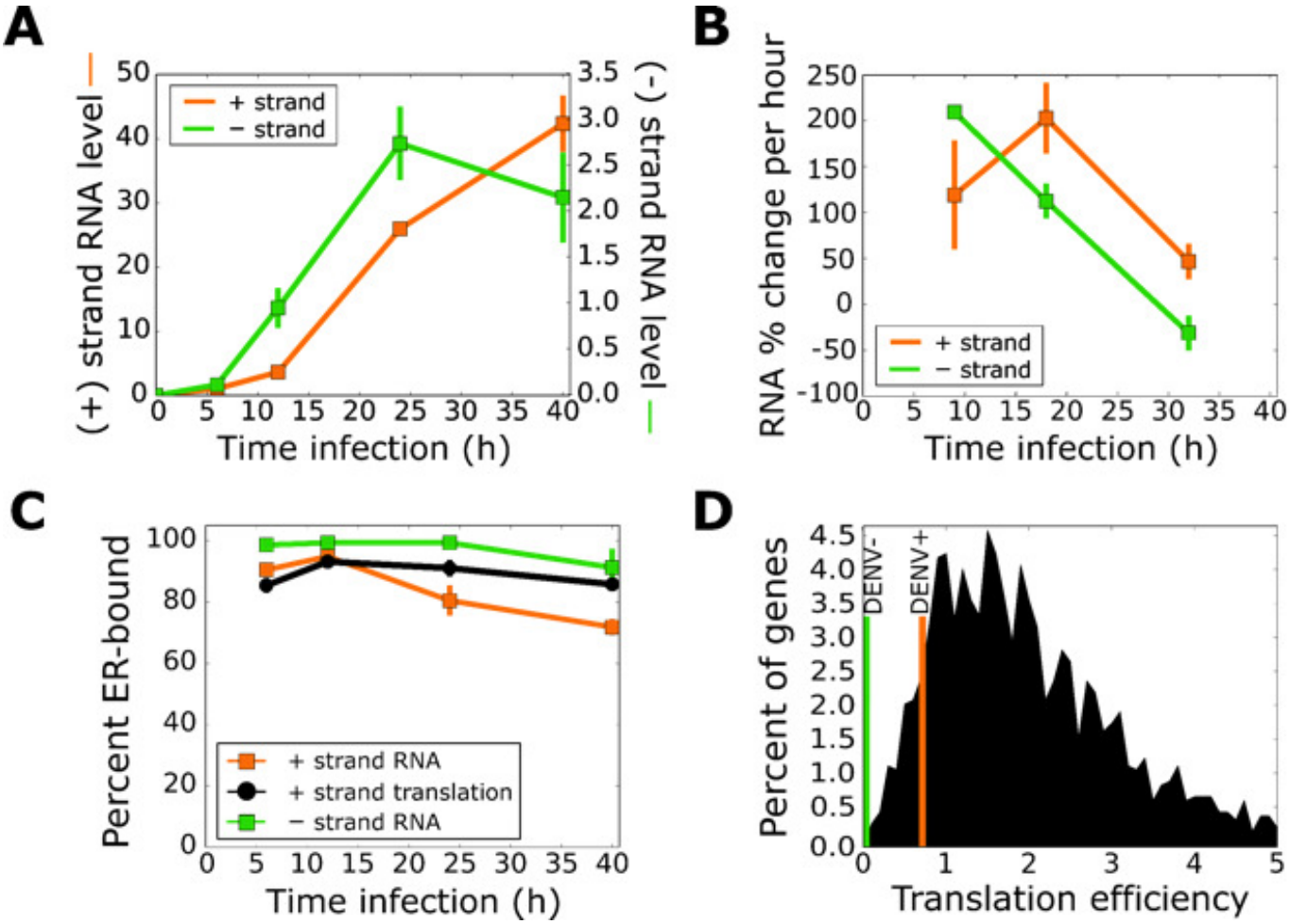

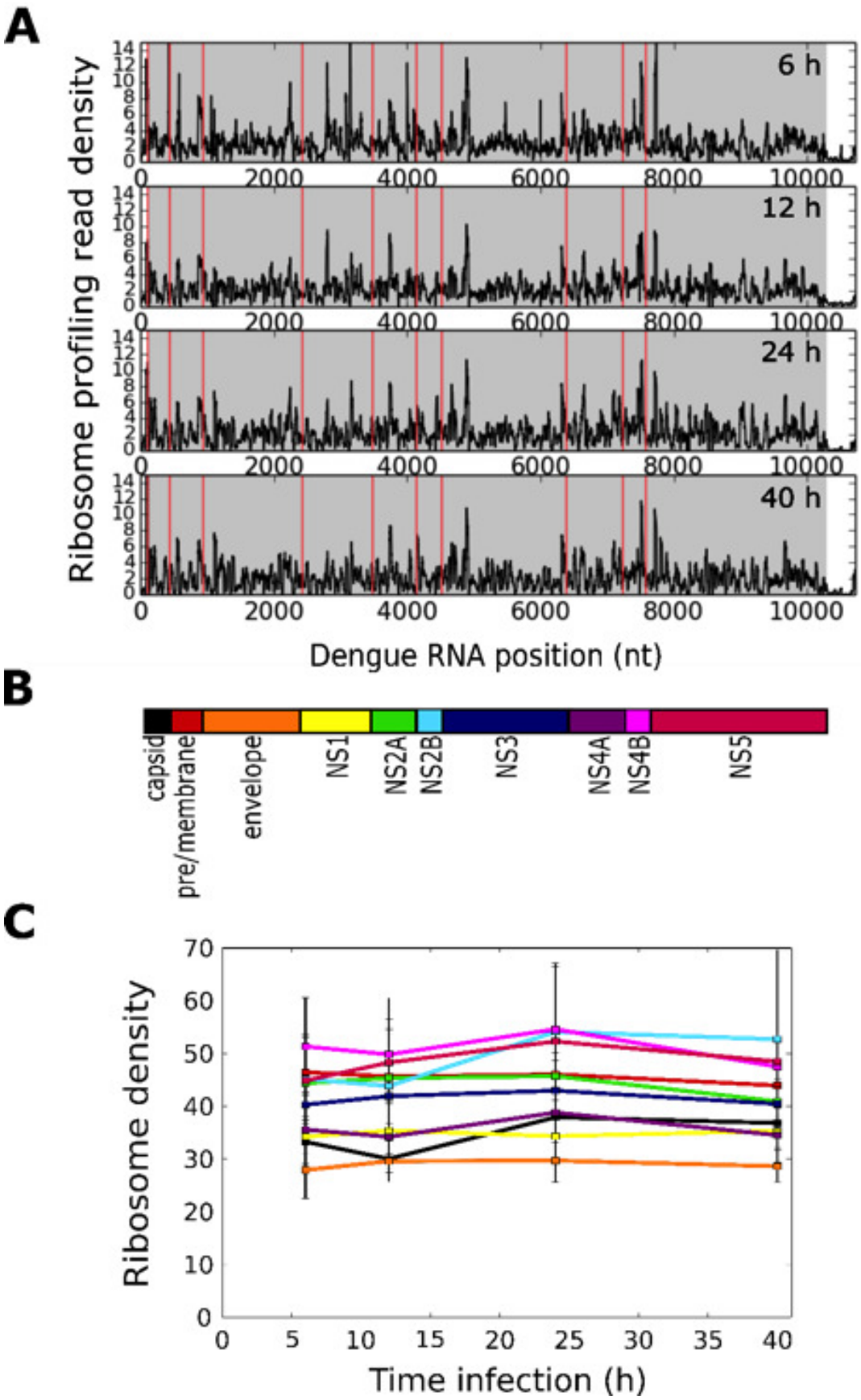

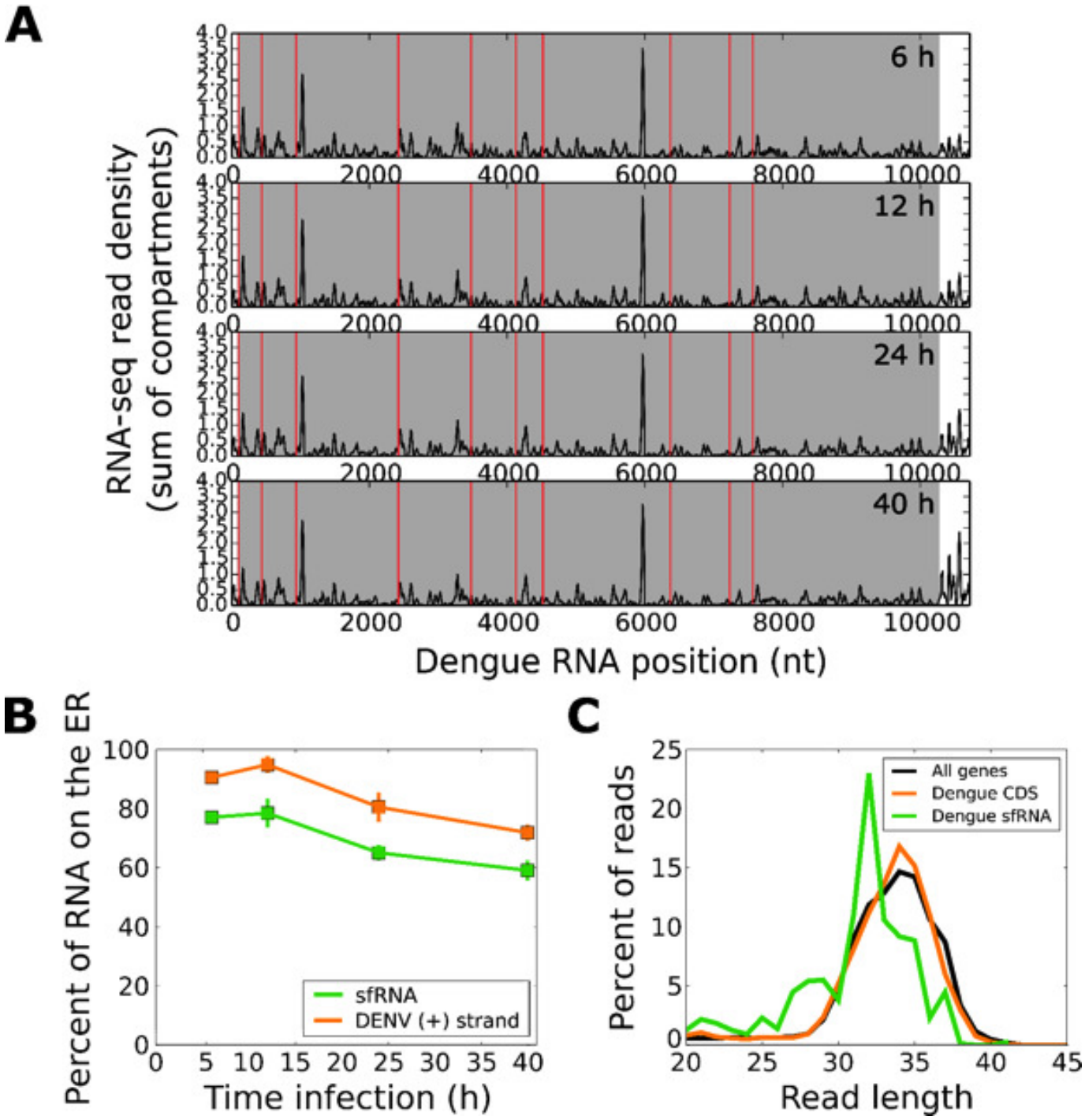

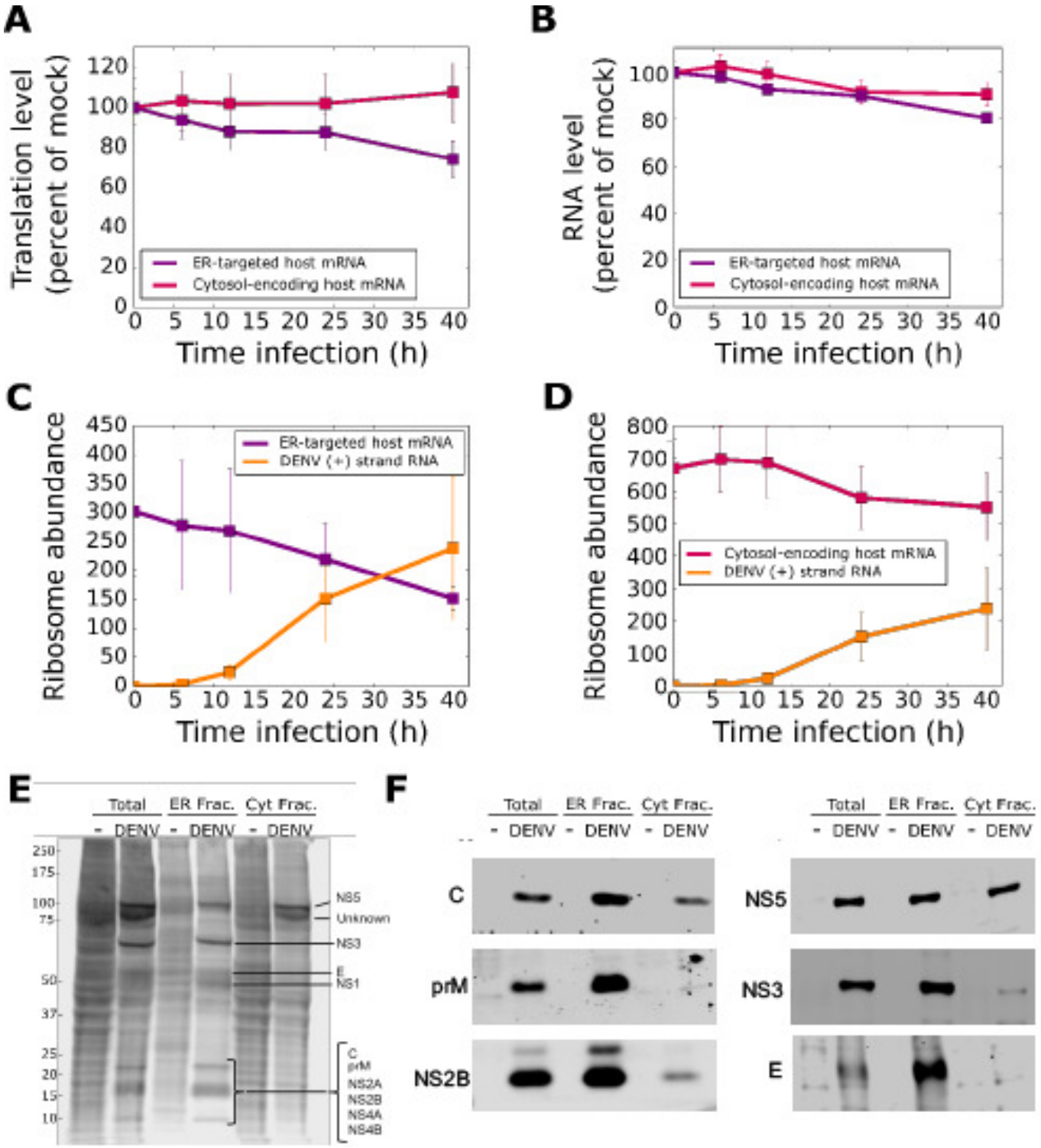

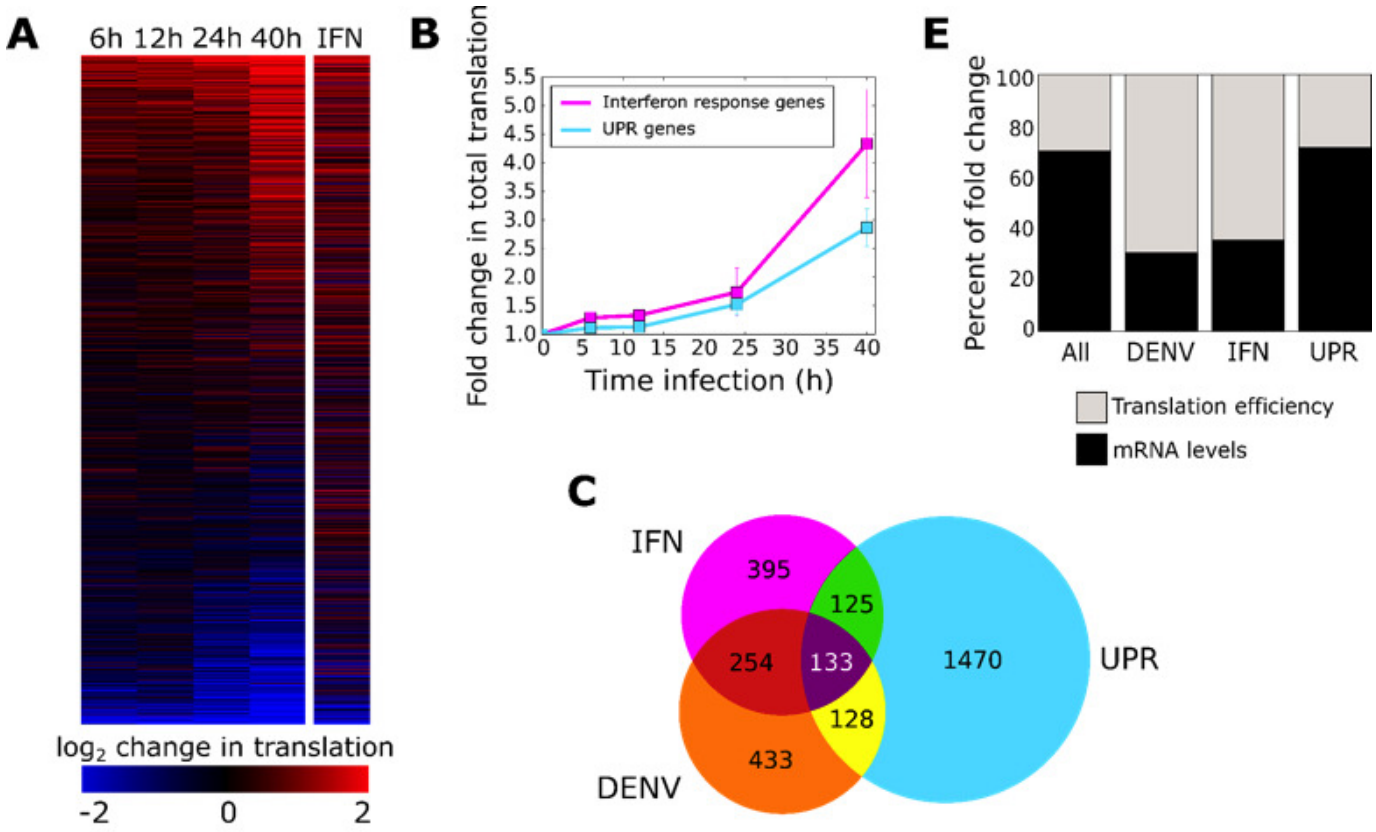

D

GO Term (biological process)	P-value	Enrichment
autophagy	7.72E-09	4.80
regulation of intracellular signal transduction	1.13E-08	2.03
regulation of GTPase activity	2.99E-08	2.74
cellular macromolecule metabolic process	2.59E-07	2.20
RNA metabolic process	7.99E-07	1.58

A

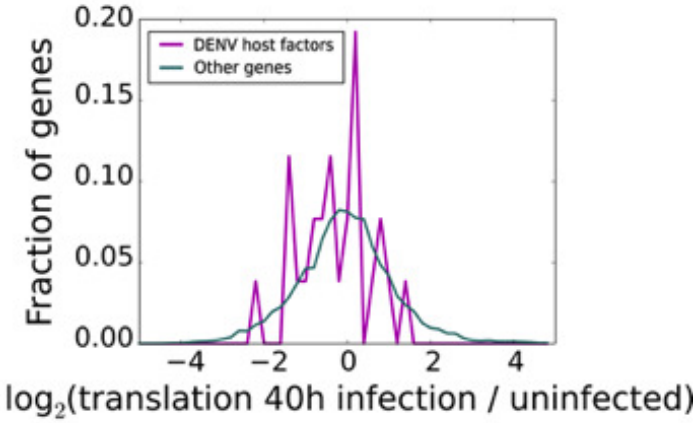

B

Gene ID	ER?	Log_2 change in total translation
CILP	No	NA
NRSN1	Yes	NA
EMC2	Yes	2.561466
TBC1D9	Yes	1.646808
TSEN15	No	1.175835
RAB5A	No	1.153792
ASCC2	No	1.129517
TTC7A	No	1.105917
LYSMD3	Yes	1.016606
ASCC3	No	0.560635
UBE2J1	Yes	0.084272
SSR3	Yes	0.02432
HSPA13	Yes	0.001863
OST4	Yes	-0.13629
MAGT1	Yes	-0.27337
SSR2	Yes	-0.36101
TTC37	No	-0.38785
SEC61A1	Yes	-0.4794
EMC3	Yes	-0.57981
LEPROT	No	-0.57992
EMC6	Yes	-0.58141
OSTC	Yes	-0.60656
DDOST	Yes	-0.74725
EMC7	Yes	-0.75134
SSR1	Yes	-0.80355
STT3A	Yes	-0.97432
SAMD8	Yes	-1.11429
MMGT1	Yes	-1.14545
EMC1	Yes	-1.20918
RPN2	Yes	-1.31322
EMC4	Yes	-1.34744
STT3B	Yes	-1.46459
SVEP1	No	-1.49111
DAG1	No	-2.31305